STRESS CORROSION OF HAZ OF HETEROGENEOUS WELDING JOINTS OF DUPLEX AND AUSTENITIC STEELS

Santina Topolska[1], Aleksander Gwiazda[2]

[1] Silesian University of Technology, Faculty of Mechanical Engineering, Department of Welding, Konarskiego 18A, 44-100 Gliwice, Poland
[2] Silesian University of Technology, Faculty of Mechanical Engineering, Department of Engineering Processes Automation and Integrated Manufacturing Systems, Konarskiego 18A, 44-100 Gliwice, Poland

Corresponding author: Santina Topolska, santina.topolska@polsl.pl

Abstract: The article presents the investigations of corrosion properties of welded heterogenous joints. These joints were made on the basis of typical duplex steel (grade 2205- X2CrNiMoCuN22-5-3 steel with the number 1.4462) and typical, low-carbon austenitic steel (grade 316L - X2CrNiMo17-12-2 steel with the number 1.4404) using the welding wire P5 (Avesta, Sweden). The aim of the research was to analyze the impact of joint type and binder material on the stress corrosion of these welded joints. These samples had a round cross section. The narrower part, in the scope of which the research was conducted, had a diameter of 5 mm and the fixing part M10. The entire sample was 133 mm long and the test piece 52 mm. Two test samples were prepared for each of the joints. The samples were mounted in the pull-off brackets so that they were immersed in the solution whose corrosive action was tested. The tests show that integranullar corrosion causes fractures at the side of the hypothetically stronger 2205 duplex steel.
Key words: Welded joints, duplex steels, CERTT method.

1. INTRODUCTION

One of the moist important issues related to joining metal sheets using welding method is the problem of properties and characteristics of welded joints, including these joints that are made between duplex steel sheets and sheets of other types of steel and alloys (Bettahar et al., 2015; Moteshakker et al., 2016). This situation is increasingly taking place in the chemical, energy, aviation, maritime and shipbuilding industries. This is due to the desire to reduce costs while maintaining appropriate corrosion resistance. In the field of work, joints made between duplex steels and austenitic steels are of interest. This is due to their certain morphological similarity and the frequency of their application. Works in this area are relatively developed in many centers in Poland and around the world (Łabanowski, 2007; Neissi et al. 2016; Reddy et al., 2008). The works of the Author (Topolska, 2016) also fall within this scope.
However, welding dissimilar materials causes several problems related to their mutual differences (Nelson et al., 1999). First, the problem is usually different metallurgical weldability of individual materials. They concern, inter alia, such properties of the joined steels as: different melting point, different crystal structure, different heat capacity or different thermal conductivity. On the other hand, from the point of view of technological weldability, the difference in thermal expansion coefficients of metals in the non-inverse joint is important. Secondly, the problems of making dissimilar joints are related to the differences in the chemical composition of the joined materials. This results in a situation where the zone between the weld and the parent material shows different chemical and physical characteristics due to a different chemical composition. Most often, this composition is unfavorable in terms of mechanical and corrosion resistance of this area. In this way, the HAZ and the fusion zone create a specific structural discontinuity in the welded joint, which is a place with a higher density of defects.
Finally, in the area of material remelting, it is necessary to point out the formation of a structure different from that of the native materials, usually with worse properties. This applies not only to the weld area, but also to the fusion zone area. Morphological changes may also arise in the HAZ area as a result of temperature-induced processes. One of the additional effects of this situation is the increased risk of cracking in the area of the welded joint at high temperatures.
Taking into account the metallurgical problems related to the performance of dissimilar joints based on duplex steel, it should be noted that they most often result in a decrease in their corrosion resistance. Such connections are particularly exposed to the effects of stress corrosion cracking. Stress corrosion cracking is a local corrosion that occurs in a material that is under constant technological or operational stress. Stress corrosion cracking occurs due to the combined effect of an aggressive environment and mechanical stress on materials susceptible to this type of corrosion. The

corrosion of welded joints is electrochemical. Failures in service conditions are usually unexpected when they occur with very little general corrosion and no visible signs of it. Due to the difficulties of early detection of the risk, the effects of stress corrosion cracking can be enormous. This premise is the cause for the investigations being the subject of this paper.

2. RESEARCH METHODOLOGY

2.1 Method

The rules for carrying out the test are contained in PN-EN ISO 7539-7 and ASTM-G 36 (SSRT method - Slow Strain Rate Test). The test consists in a gradual increase in the material load in the tensile test with a controlled increase in the sample elongation. The tested samples are placed in an aggressive environment specific for a given material (Figure 1). It was specially designed test stand in the Welding Department. It containis a chamber with agrressive agent in which is placed the specimen. Endings of the specimen are mounted in the electromechanical tensile device, which operation is controlled. Stress corrosion is revealed only in a certain range of strain rate and therefore, it is typically used in the range of strain rate of 10^{-4} to 10^{-7} s^{-1}. The test is always positive as it is carried out until the test material fails.

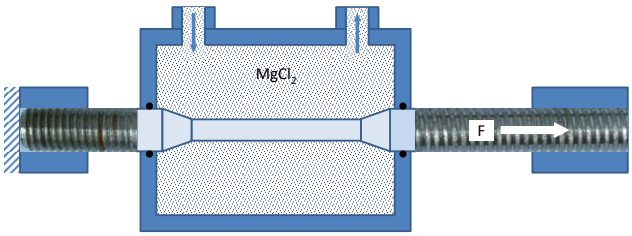

Fig. 1. Scheme of the SSRT testing, [own elaboration]

This method is mainly used for comparative trials. The test results do not provide information on the behavior of the material in real operating conditions.

2.2 Welded materials

For the test were used specimens obtained from heterogeous welded joints. These joints were manufactured using automatic submerged arc welding (SAW) technology. They were made of 2205 (0.027% C, 0.41% Si, 0.8% Mn, 22.8 % Cr. 5.33% Ni, 3.11% Mo, 0.16% N – according delivery certificate) and 316L (0.041% C, 0.52% Si, 1.69% Mn, 17.2 % Cr, 9.9% Ni, 2.1% Mo, 0.04% N – according delivery certificate) steel sheets.
Welding process was performed using the 3.2 mm P5 welding wire of Avesta (0.009% C, 0.32% Si, 1.4% Mn, 21.2 % Cr, 15.1% Ni, 2.62% Mo, 0.06% N – according delivery certificate). This wire characterizes with the austenitic structure containing 5 - 10% of ferrite (EN ISO 14343: S 23 12 2 L, AWS A5.9: ER309LMo). The ferrite number for the P5 welding wire is 8 (according deLong diagram) or 9 (according the WRC-92 diagram). Values of the heat input, during welding, varied for the weld No 2A from 1.19 kJ/mm up to 3.64 kJ/mm for the weld No 2B.

2.3 Specimens

For the research, four types of butt joints were prepared. They are divided into two groups: two-pass welds and multiple-pass welds. The samples for the stress corrosion impact test (SSRT) were taken from the central part of the sheet metal sections, as shown in Figure 2. In this figure is shown the simplified cross-section of welded joints. From this are were cut the samples (yellow area plus surplus for turning) and then turned on the lathe to obtaing the cylindrical form. The endings were threading to mount the samples in the holder of the tensile machine.

Fig. 2. Location of the specimen, [own elaboration]

In Figure 3 are presented approximate locations of individual samples for the SSRT testing. It is shown in front of the entire heteregenous welded joint. The left side is the 2205 steel and the right side is the 316L steel side. As it is visible the samples represent the central part of the joint.

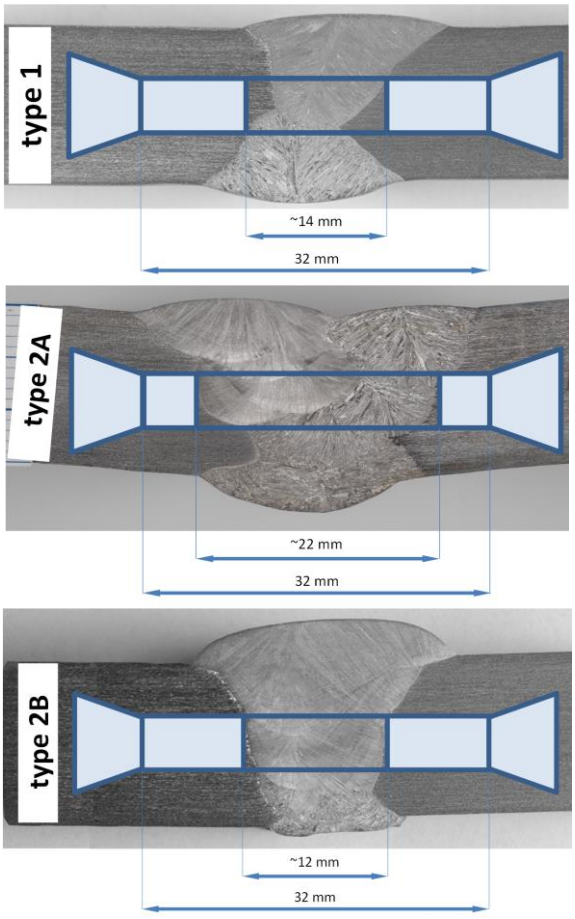

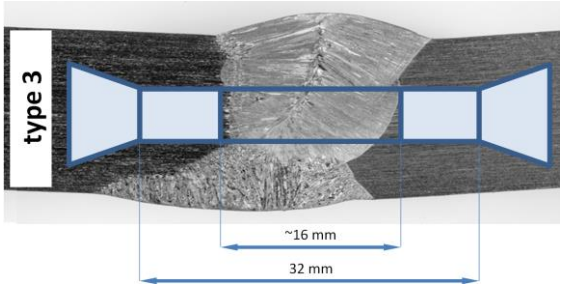

Fig. 3. Locations of specimens, [own elaboration]

The Type 1 represents the two-passes, I-type weld. Type 2A is the multi-passes, Y type weld with limited to 1.5 kJ/mm welding energy and Type 2B is the same one but withait limited welding energy. The Type 3 is two-passes, 2Y-type weld.
These samples had a circular cross-section. The narrower part, in the scope of which the tests were carried out, had a diameter of 5 mm and the mounting part M10. The length of the entire sample was 133 mm and the test piece 52 mm. This type of testing, including samples geometry is discussed in [Top17b]. Two test specimens were prepared for each of the joints. The samples were mounted in the ripper's holders so that they were immersed in the solution, the corrosive effect of which was tested. The parameters recorded during the test were force (F) and elongation (A), with the elongation speed being a constant, controlled value of the order of $2x10^{-6}$ 1 / s. After the test, the remaining test parameters were determined (the narrowing Z and the energy of destruction of the E_Z sample as well as the point of fracture). The working length of the sample was L_0 = 32 mm, its working diameter was d_0 = 5 mm, and the working volume V_r = 630 mm^3 ($6.3x10^{-7}$ m^3).
It was also indicated what scope, in the case of individual samples, was occupied by the weld and what scope was tested.

3. TESTING RESULTS

The parameters determined on the basis of the results of the SSRT test in the $MgCl_2$ solution with a constant temperature of 125°C, at a constant strain rate, are presented in Tab. 1. Secondary values were determined on the basis of primary research results. For comparison purposes, tear tests were performed on the samples placed in the neutral environment of $C_3H_8O_3$, while maintaining all the conditions of the first test (tensile speed and environmental temperature). The obtained results are presented in Table 2. Is is interesting to compare the side of fracture of particular samples.

Table 1. Main results of the CERTT test in $MgCl_2$ (corrosive) environment, [own elaboration]

	Type 1 Specimen 1	Type 1 Specimen 2	Type 2A Specimen 1	Type 2A Specimen 2	Type 2B Specimen 1	Type 2B Specimen 2	Type 3 Specimen 1	Type 3 Specimen 2	2205	316L
Total elongation $\varepsilon=\Delta L/L_0$	0.123	0.321	0.096	0.129	0.072	0.081	0.084	0.247	0.230	0.281
Maximum breaking strength F_m [kN]	5.395	9.702	6.719	8.134	6.302	6.424	6.695	9.909	10.238	9.129
Tensile strength R_m [MPa]	274.0	492.8	341.3	413.2	320.1	326.3	340.1	503.3	520.0	463.7
Testing duration T [s]	74790	198990	60480	84870	44100	52650	52200	152640	110070	179820
Relative stretching speed v/L_0 [1/s]	1.64 x 10^{-6}	1.61 x 10^{-6}	1.58 x 10^{-6}	1.52 x 10^{-6}	1.63 x 10^{-6}	1.54 x 10^{-6}	1.61 x 10^{-6}	1.62 x 10^{-6}	2.09 x 10^{-6}	1.56 x 10^{-6}
Break energy E_Z [J]	16.31	51.83	15.94	27.66	10.88	13.65	13.29	62.97	34.69	58.54
Relative energy of fracture E_Z/V_r [MJ/m^3]	25.97	82.49	25.37	44.02	17.32	21.73	21.15	100.22	88.34	99.37
Place of fracture (side of the specimen)	2205	316L	2205	2205	2205	2205	2205	316L	middle	middle

Table 2. Main results of the CERTT test in $C_3H_8O_3$ (neutral) environment, (own elaboration)

	Type 1	Type 2A	Type 2B	Type 3	2205	316L
Total elongation $\varepsilon=\Delta L/L_0$	0.328	0.271	0.333	0.330	0.452	0.431
Maximum breaking strength F_m [kN]	9.775	9.907	10.054	9.431	12.366	9.543
Tensile strength R_m [MPa]	496.5	503.2	510.7	479.0	628.1	484.7
Testing duration T [s]	200250	168930	205020	202320	221040	267390
Relative stretching speed v/L_0 [1/s]	1.64 x 10^{-6}	1.60 x 10^{-6}	1.62 x 10^{-6}	1.63 x 10^{-6}	2.04 x 10^{-6}	1.61 x 10^{-6}
Break energy E_Z [J]	64.82	47.97	62.61	53.23	92.79	102.80 J
Relative energy of fracture E_Z/V_r [MJ/m^3]	103.18	76.35	99.64	84.73	236.30	174.52
Place of fracture (side of the specimen)	316L	316L	316L	316L	left side	left side

The test results in the form of diagrams showing the places of cracking of the specimens are shown in Figure 4. The photos of the samples are on the bottom right. Figure 5 shows schematically the breaking points of samples made of 2205 steel (tested in both analyzed environments). On the other hand, this figure shows schematically the places where the samples made of 316L steel have broken.

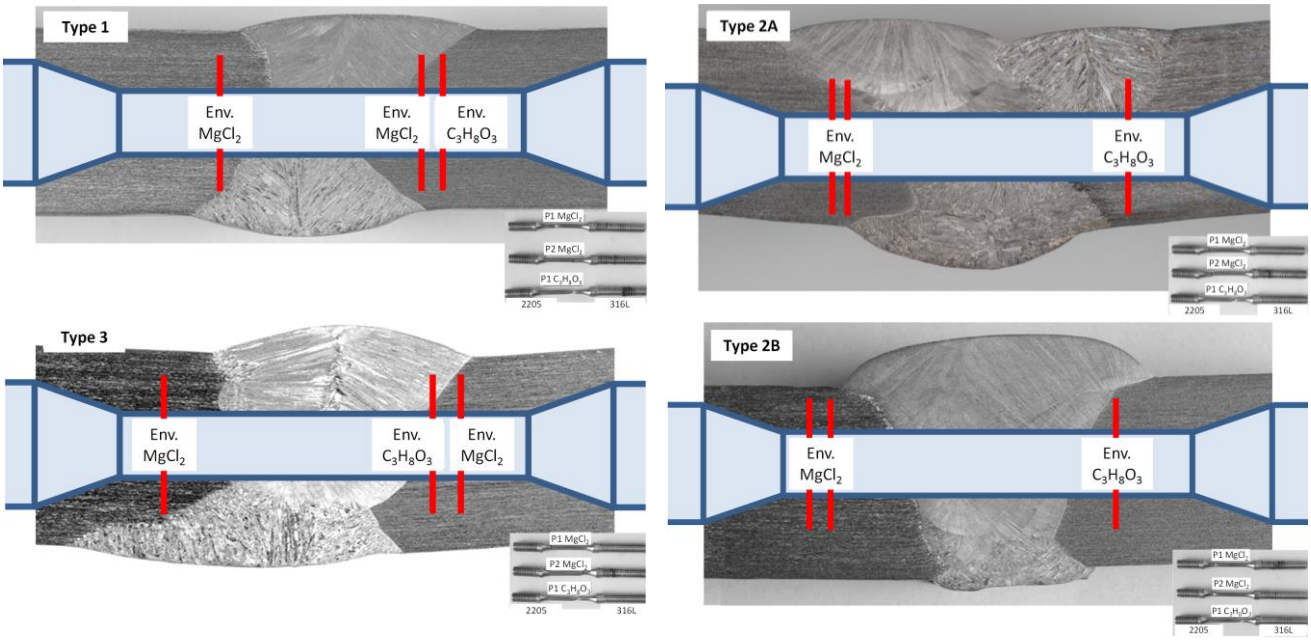

Fig. 4. Specimens fracture locations for different joint type, [own elaboration]

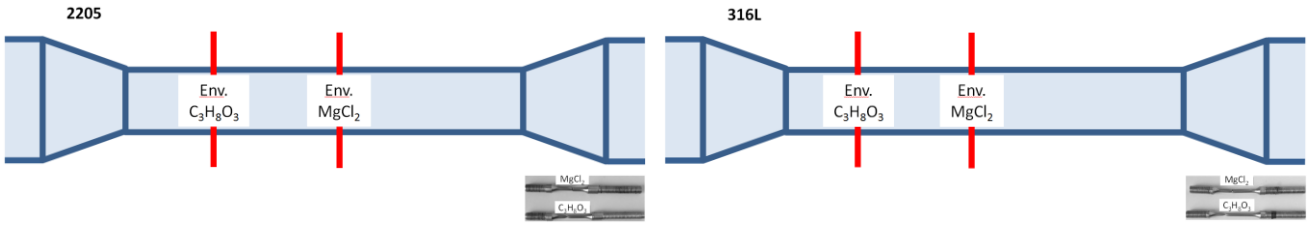

Fig. 5. Fracture locations for specimens made from 2205 and 316L steels, [own elaboration]

The obtained results allow for the formulation of specific conclusions from the trials, but also force us to formulate several theses regarding the mechanisms, the effects of which could be observed. Firstly, the influence of the corrosive environment on the obtained test results is clearly visible. Comparison of the results obtained in the corrosive environment ($MgCl_2$) and in the neutral environment ($C_3H_8O_3$). It shows significant differences in the cracking mechanism of the samples. In a corrosive environment, cracking occurs at a lower elongation value, which indicates a higher brittleness of the material. In the case of samples of welded joints, in a corrosive environment, the mean values of elongation and reduction are indicated.

The indicated comparison shows a decrease in the value of elongation A, in the case of samples of welded joints tested in a corrosive environment, by half as compared to the results for the inert environment (from 32 to 17% on average). A similar observation can be made in the case of narrowing Z. However, in this case the decrease is 1/3 (from an average of 76 to an average of 26%). Thus, the statement about the negative influence of the corrosive environment on the properties of the mechanical properties of the tested type of dissimilar joints should be indicated as corrected.

Comparing the individual results with each other, one should pay attention to a significant decrease in the value of elongation A in the case of the type 2B joint, taking into account that in the neutral environment. The values of this parameter were similar to its values also for the type 1 and type 3 joints and type 2A joints. Taking this observation into account, it should be stated that the tested multi-run welded joints, in this respect, are more susceptible to stress corrosion cracking than double-run joints. However, limiting the welding energy improves this situation (joint 2A). Additionally, a comparison with the elongation values for native materials shows a noticeable decrease of this parameter for the tested welded joints, regardless of the nature of the environment. On the other hand, in the case of constriction Z, the nature of the changes is less acute. However, it can be

stated that it reflects the observations concerning the elongation characteristics.

For comparison purposes, it is possible to show diagrams taking into account data only for cracks on the side of 2205 steel. There is a decrease in the plasticity measured in the case of type 1 and type 3 joint samples, in which occurred the second fracture on the 316L side. In the case of elongation testing for type 1 and type 2A joint samples, the yield loss at fracture on the 2205 steel side is clearly lower than in the case of type 2B and type 3 joint samples. However, in the case of the throat diagram, these characteristics are not so clearly outlined. Probably in this case the large share of austenite in the weld cross-section (joint 1) and lower welding energies (joint 2A) are decisive.

In the case of tensile strength analysis, its decrease can be observed for all samples placed in a corrosive environment. The smallest values are for samples of the type 3 joint (by 12%), and for the base material for the sample made of 316L steel (by 4%). The biggest decrease should be noted for samples of the type 2B connector (by 37%). Also, in general, multi-pass couplings turn out to be on average worse than double-pass couplings. This tendency is better observed in the case of EZ destruction energy. The decrease in the value of this parameter for the samples of the type 3 joint is 28%, and in the case of the samples of the type 2B joint it is as much as 80%. In the case of this parameter, the multi-pass connectors turn out to be clearly worse. Noteworthy is also a large drop in energy of failure for native materials (2205 steel by 63% and 316L steel by 43%). Also it was an attempt conducted to model the SSRT testing. In Figure 6 is presented one of results of a try to virtually model the SSRT testing. The models were prepared in NX PLM (Siemens, Germany) platform using data from material tests. Then it was simulated the process of very slow stretching. The results, however, was only close to actual ones. The next investigations are directed to searching the method of modeling the influence environment,

As a result of these studies, the occurrence of M23C6 carbide precipitates (lamellar plates) was found in the area of high-chromium ferrite grains (most often at their borders). It should be pointed out that the average content of Cr in ferrite is about 4% higher than in austenite. In Figure 7 are presented the microscopic images of SWC 2205 and SWC 316L. It shows an increased intensity of the indicated precipitates and their larger sizes on the side of HAZ of 2205 steel.

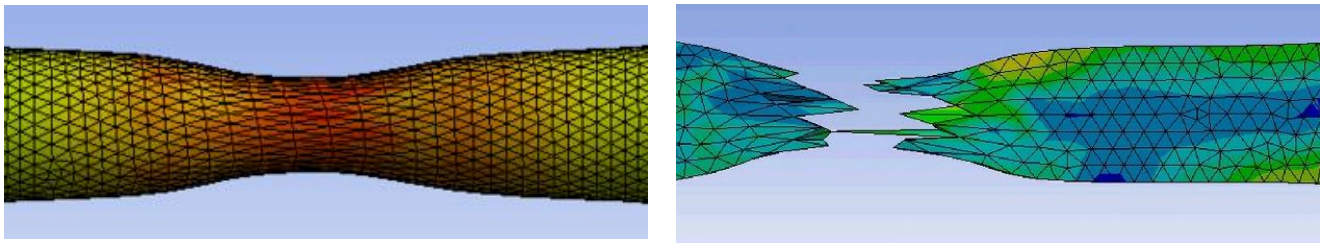

Fig. 6. Model of virtual analysis, [own elaboration]

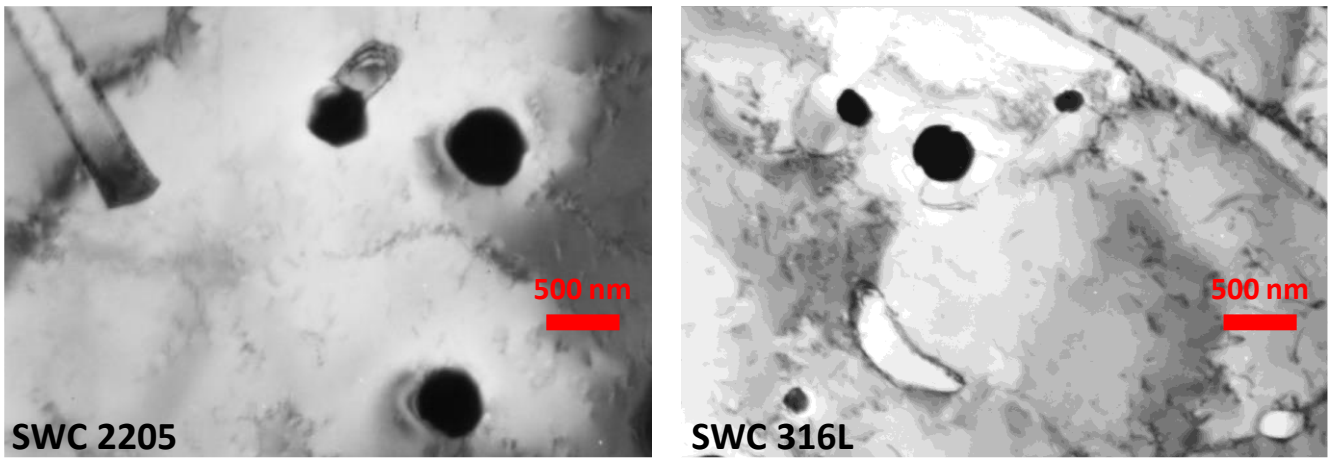

a) b)

Fig. 7. $M_{23}C_6$ carbide particles on the side: a) HAZ 2205, b) HAZ 316L of the type 3 joint, [own elaboration]

5. CONCLUSIONS

The presented results show, on the one hand, that there are reasons to distinguish, in terms of the presented analysis, type 2A and type 3 joints, which suggests a positive impact of linear energy limitation on the one hand, and a positive effect of the weld geometry in type 2Y, on the other.

In addition, attention should be paid to the change in the characteristics of type 1 and type 3 joints, taking into account only the cracks from the 2205 steel side. This suggests the existence of two separate crack mechanisms: one for cracks on the 2205 side (generally at lower parameters) and the other for cracks on the side of 316L steel (with higher parameters). For example, for a type 1 specimen, the tensile strength for 2205 side fracture was 274 MPa and for 316L side fracture was 493 MPa, which is 180% of the former, or else 55% of the latter. For samples for a Type 3 joint, the first value is 68% of the second value. These are already significant differences in values confirming the existence of two separate fracture mechanisms. Taking this into account, it can be indicated that in the case of cracks on the side of 2205 steel, their occurrence at low parameter values is probably due to precipitation in the ferrite region, which is significantly eroded in a corrosive environment. It should be recalled that the share of ferrite on the side of 2205 steel is at the level of 70%. In an inert environment, however, they only partially limit the parameters of the tested joints, if at all, in relation to the native materials. Additionally, it can be concluded, based on the analysis of the indicated sample parameters that in the case of multi-pass welds (type 2A and especially type 2B). The indicated mechanism is more intense due to the multiplication of the number of thermal cycles compared to double-pass welds. Taking this into account, it was found necessary to perform additional tests on a transmission microscope, the purpose of which is to determine the type and, if possible, intensity of the occurrence of the sought precipitates.
Basing on the presented results it is planned to elaborate the method of modeling the dissimilar joints of this type (duplex – austenitic steels) to predict its future properties.

6. REFERENCES

1. Bettahar K., Bouabdallah M., Badji R., Gaceb M., Kahloun C., Bacroix B., (2015). *Microstructure and mechanical behavior in dissimilar 13Cr/2205 stainless steel welded pipes*, Materials and Design, **85**, 221–229.
2. Łabanowski J., (2007). *Mechanical properties and corrosion resistance of dissimilar stainless steel welds*, Archives of Materials Science and Engineering, **28**(1), 27-33.
3. Moteshakker A., Danaee I., (2016). *Microstructure and Corrosion Resistance of Dissimilar Weld-Joints between Duplex Stainless Steel 2205 and Austenitic Stainless Steel 316L*, Journal of Materials Science & Technology, **32**, 282-290.
4. Neissi R., Shamanian M., Hajihashemi M., (2016). *The effect of constant and pulsed current gas tungsten arc welding on joint properties of 2205 duplex stainless steel to 316L austenitic stainless steel*, Journal of Materials Engineering and Performance **25**(5), 2017-2028.
5. Nelson T. W., Lippold J. C., Mills M. J., (1999). *Nature and evolution of the fusion boundary in ferritic-austenitic dissimilar weld metals*. Part 1: Nucleation and growth, Welding Journal, **78**, 329–337.
6. Reddy G. M., Rao K. S., Sekhar T., (2008). *Microstructure and pitting corrosion of similar and dissimilar stainless steel welds*, Science and Technology of Welding and Joining, **13**(4), 363-377.
7. *The Avesta Welding Manual, Practice and products for stainless steel welding*. Available from: http://www-eng.lbl.gov/~shuman/NEXT/MATERIALS&COMPONENTS/Pressure_vessels/ss_weld_manual_avesta.pdf. Accessed: 11/04/2019.
8. Topolska S., (2016). *Hardness analysis of welded joints of austenitic and duplex stainless steels*, IOP Conference Series: Materials Science and Engineering, **145**, 272-277.

Received: April 12, 2020 / Accepted: December 20, 2020 / Paper available online: December 25, 2020